Available online at www.sciencedirect.com
ScienceDirect
Journal of Solid State Chemistry 179 (2006) 3628–3635
JOURNAL OF SOLID STATE CHEMISTRY
www.elsevier.com/locate/jssc

A hybrid material based on $[Mo_6Br_{14}]^{2-}$ inorganic cluster units and $[BEDO\text{-}TTF]^{+}$ organic monocationic radicals: Synthesis, structure and properties of $(BEDO\text{-}TTF)_2Mo_6Br_{14}(PhCN)_4$

Kaplan Kirakci[a], Hidemasa Hosoda[b], Stéphane Cordier[a], Christiane Perrin[a,*,1], Gunzi Saito[b,*,2]

[a]*UMR CNRS 6226 "Sciences Chimiques de Rennes", Université de Rennes 1, Campus de Beaulieu (Bât. 10A), Avenue du Général Leclerc, 35042 Rennes Cedex, France*
[b]*Organic Solid State Chemistry, Division of Chemistry, Graduate School of Science, Kyoto University, Oiwake-cho, Kitashirakawa, Sakyo-ku, Kyoto, 606-8502, Japan*

Received 16 December 2005; received in revised form 18 July 2006; accepted 22 July 2006
Available online 7 September 2006

Abstract

The first charge transfer salt based on non- dimerized $[BEDO\text{-}TTF]^{+}$ monocationic radical (BEDO-TTF = bis(ethylenedioxy)tetrathiafulvalene) associated with $[Mo_6Br_{14}]^{2-}$ cluster anions has been synthesized by conventional electro-oxidation and characterized by single crystal X-ray diffraction, UV–VIS–NIR absorption and magnetic susceptibility measurements. $(BEDO\text{-}TTF)_2Mo_6Br_{14}(PhCN)_4$ crystallizes in the monoclinic system, space group $P2_1/n$, $a = 10.414(4)$ Å, $b = 21.711(7)$ Å, $c = 15.958(5)$ Å, $\beta = 93.65(3)^\circ$, $V = 3601(2)$ Å^3, $Z = 2$, $R_1 = 0.0578$, w$R_2 = 0.0731$. The structure of this hybrid compound is built up from a $[BEDO\text{-}TTF]^{+}$ and PhCN (benzonitrile) organic framework in which are hosted the $[Mo_6Br_{14}]^{2-}$ inorganic cluster units. It results in non- dimerized $[BEDO\text{-}TTF]^{+}$ cations that exhibit a paramagnetic behavior characteristic of one unpaired electron.

Keywords: Molybdenum; Octahedral cluster; Electro-oxidation; BEDO-TTF cation; Crystal structure; X-ray diffraction; UV–VIS–NIR spectroscopy; Magnetism

1. Introduction

Low oxidation state molybdenum halides and chalcohalides are well known to form $Mo_6L^i_8L^a_6$ cluster units, with metal–-metal bonds, in which the Mo_6 cluster is face capped by eight inner ligands (L^i) to form a $Mo_6L^i_8$ core additionally bonded to six apical ligands (L^a) (^{a} = apical, ^{i} = inner according to the Schäfer and von Schnering notation [1]). Within the solid, these units can be discrete or interconnected by shared inner and/or apical ligands leading to stronger electronic interactions. It results in compounds with various dimensionalities (condensation of units along one, two or three directions of the space) [2] and with a wide range of physical properties such as superconductivity at high critical field [3], catalytic [4] or intercalation [5] behavior. On the other hand, compounds based on discrete units exhibit insulating properties related to a strong molecular character of the unit.

Inorganic solid-state Mo_6 cluster compounds based on discrete units constitute relevant precursors for the elaboration of organic/inorganic or organometallic/inorganic hybrid materials via solution chemistry route [6]. The solubility of units can be increased through cationic metathesis by the exchange in solution of inorganic cations as for instance Cs^+ in $Cs_2Mo_6X_{14}$ series by $(Bu_4N)^+$ to yield $(Bu_4N)_2Mo_6X_{14}$ (X = Cl, Br, I). Hybrid cluster materials can be prepared according to two approaches: (*I*) crystallization of cluster anionic units with organic or hybrid organic/inorganic counter cations [7], (*II*) functionalization of Mo_6 cluster by organic or hybrid organic/

*Corresponding authors.
E-mail addresses: christiane.perrin@univ-rennes1.fr (C. Perrin), saito@kuchem.kyoto-u.ac.jp (G. Saito).
[1]Fax: +33 2 23 23 67 99.
[2]Fax: +81 75 753 4035.

0022-4596/$ - see front matter © 2006 Elsevier Inc. All rights reserved.
doi:10.1016/j.jssc.2006.07.030

inorganic ligands in apical position [8]. Both of them have been investigated in molybdenum chloride chemistry, and more recently with iodides and bromides resulting in original Mo_6-cluster-cored 18-silylferrocenyl dendrimer $(Bu_4N)_2[Mo_6Br_8(OC_6H_4C(C_3H_6SiC_2H_6Fc)_3)_6]$ (where Fc is ferrocen) [9] or in the $[Cp^*(dppe)Fe\text{-}NCMe]_2.M_6L_{14}$ series obtained from the crystallization of inorganic $[M_6L_{14}]^{2-}$ anionic cluster units with $[Cp^*(dppe)Fe\text{-}NCMe]^+$ organometallic entities as the cationic counter cation (Cp^* = pentamethylcyclopentadienyl, dppe = 1,2-bis(diphenylphosphino)ethane) [10]. In this work, we report the synthesis of a hybrid material, namely $(BEDO\text{-}TTF)_2Mo_6Br_{14}(PhCN)_4$ (BEDO-TTF = bis(ethylenedioxy) tetrathiafulvalene, PhCN = benzonitrile). It has been known that BEDO-TTF radicals have a strong self-assembling nature to afford two-dimensional electronic structures of the charge transfer salts [11]. The origin of this property is regarded as the molecular shape of BEDO-TTF and the intermolecular atomic arrangement, namely the CH···O hydrogen bonds along the face-to-face direction and robust transfer interactions arising from the strong sulfur···sulfur atomic contacts along the side-by-side direction. As a result, a stable two-dimensional electronic structure with a wide bandwidth has been formed in many cation radical salts regardless of the kind, shape and size of acceptor or anion molecules. Here we found the first charge transfer salt based on non- dimerized BEDO-TTF monocationic radicals that have been stabilized by the use of $[Mo_6Br_{14}]^{2-}$ cluster units as counter anions. The influence of the $[Mo_6Br_{14}]^{2-}$ inorganic cluster units on the BEDO-TTF/PhCN organic framework organization in relation to the physical properties will be

Table 1
Crystallographic data for the structure determination of $(BEDO\text{-}TTF)_2Mo_6Br_{14}(PhCN)_4$

Empirical formula	$C_{48}H_{36}Br_{14}Mo_6N_4O_8S_8$
Formula weight	2747.6
Space group	$P\,2_1/n$ No. 14
a (Å)	10.414(4)
b (Å)	21.711(7)
c (Å)	15.958(5)
β (°)	93.65(3)
V (Å^3)	3601(2)
Z	2
D_{calc},g cm^{-3}	2.534
Crystal dimensions (mm^3)	$0.015 \times 0.020 \times 0.060$
Total reflections collected	8900
Unique reflections	6327
R_{int} (all reflections)	0.0242
μ (mm^{-1})	9.054
T (°C)	20
λ (Å)	0.71073
Observed reflections [$I>2\sigma$ (I)]	3130
Refined parameters	397
R_1,[a] [$I>2\sigma$ (I)]	0.0578
wR_2,[a] all data	0.0731
$\Delta\rho_{min}/\Delta\rho_{max}$ (e Å^{-3})	−0.686/0.708

[a] $R_1 = \Sigma_{hkl}|F_o-F_c|/\Sigma_{hkl}|F_o|$; $wR_2 = [\Sigma_{hkl}[w(F_o^2-F_c^2)^2]/\Sigma_{hkl}[w(F_o^2)^2]]$.

Table 2
Atomic coordinates and isotropic equivalent displacement parameters (Å^2) for $(BEDO\text{-}TTF)_2Mo_6Br_{14}(PhCN)_4$

Atom	x	y	z	U_{eq}
Mo1	0.84399(12)	0.45976(6)	0.51201(8)	0.0298(3)
Mo2	0.93035(12)	0.53955(6)	0.40378(8)	0.0293(3)
Mo3	0.05260(12)	0.43515(5)	0.43364(8)	0.0294(3)
Br1	0.63043(14)	0.40057(7)	0.52816(11)	0.0473(4)
Br2	0.84117(16)	0.59468(7)	0.26762(10)	0.0513(5)
Br3	0.11639(17)	0.34535(7)	0.33820(11)	0.0510(5)
Br4	0.82795(14)	0.43617(7)	0.35180(9)	0.0370(4)
Br5	0.02942(15)	0.64294(6)	0.45834(10)	0.0378(4)
Br6	0.13816(14)	0.51395(7)	0.32814(10)	0.0387(4)
Br7	0.27508(14)	0.43616(7)	0.51751(9)	0.0380(4)
C1	0.348(2)	0.2824(13)	0.8969(14)	0.134(11)
H1A	0.4147	0.2616	0.9303	0.161
H1B	0.3277	0.3189	0.9272	0.161
C2	0.246(3)	0.2468(12)	0.8958(14)	0.127(10)
H2A	0.1773	0.2722	0.9138	0.152
H2B	0.2629	0.2168	0.9393	0.152
C3	0.2480(17)	0.2338(8)	0.7585(13)	0.057(5)
C4	0.3471(17)	0.2719(7)	0.7567(12)	0.057(5)
C5	0.2949(16)	0.2421(7)	0.6038(12)	0.060(5)
C6	0.2960(16)	0.2335(7)	0.5186(12)	0.060(5)
C7	0.3513(17)	0.2329(7)	0.3672(12)	0.052(5)
C8	0.2522(17)	0.1955(8)	0.3688(12)	0.062(5)
C9	0.243(3)	0.1880(14)	0.2314(16)	0.160(14)
H9A	0.2405	0.1551	0.1911	0.191
H9B	0.1807	0.2179	0.2108	0.191
C10	0.354(2)	0.2134(13)	0.2291(14)	0.126(10)
H10A	0.3491	0.2404	0.1814	0.151
H10B	0.4132	0.1814	0.2173	0.151
O1	0.4033(11)	0.3019(5)	0.8232(8)	0.063(3)
O2	0.1951(11)	0.2146(6)	0.8273(9)	0.074(4)
O3	0.1978(12)	0.1638(6)	0.3044(9)	0.085(4)
O4	0.4114(11)	0.2484(6)	0.2991(9)	0.075(4)
S1	0.4036(5)	0.2898(2)	0.6592(3)	0.0671(14)
S2	0.1879(5)	0.2040(2)	0.6631(4)	0.0826(17)
S3	0.1854(5)	0.1874(2)	0.4659(4)	0.0753(16)
S4	0.4059(4)	0.2697(2)	0.4591(3)	0.0606(14)
C21	0.5098(17)	0.4998(9)	0.8196(11)	0.062(5)
C22	0.4921(15)	0.4790(7)	0.7371(12)	0.054(5)
H22	0.4658	0.4378	0.7230	0.065
C23	0.5156(15)	0.5229(8)	0.6774(11)	0.059(5)
H23	0.5042	0.5122	0.6190	0.071
C24	0.5542(17)	0.5804(9)	0.6989(13)	0.071(6)
H24	0.5714	0.6091	0.6554	0.085
C25	0.569(2)	0.5987(10)	0.7800(13)	0.092(7)
H25	0.5932	0.6405	0.7934	0.110
C26	0.5507(18)	0.5573(7)	0.8427(13)	0.073(6)
H26	0.5659	0.5684	0.9007	0.088
C27	0.484(2)	0.4583(10)	0.8879(15)	0.091(7)
N1	0.463(2)	0.4217(8)	0.9461(13)	0.142(9)
C31	0.016(2)	0.3897(10)	0.0485(15)	0.079(7)
C32	0.949(2)	0.4119(10)	0.1142(15)	0.095(8)
H32	0.9733	0.4001	0.1710	0.115
C33	0.846(3)	0.4511(11)	0.0976(19)	0.121(11)
H33	0.7974	0.4662	0.1426	0.145
C34	0.813(3)	0.4683(11)	0.017(2)	0.112(9)
H34	0.7418	0.4957	0.0049	0.134
C35	0.882(3)	0.4462(10)	0.9523(16)	0.091(8)
H35	0.8580	0.4579	0.8954	0.110
C36	0.981(2)	0.4088(10)	0.9684(14)	0.078(7)
H36	0.0300	0.3948	0.9230	0.094
C37	0.123(3)	0.3498(12)	0.0653(15)	0.085(8)
N2	0.212(2)	0.3185(10)	0.0773(13)	0.111(7)

Table 3
Relevant interatomic distances (Å) in $(BEDO\text{-}TTF)_2Mo_6Br_{14}(PhCN)_4$

Cluster unit			
Mo–Mo	*Average 2.637*		
	Range: 2.628(2)–2.647(2)		
Mo–Br^a	*Average 2.594*		
	Range: 2.587(2)–2.600(2)		
Mo–Br^i	*Average 2.603*		
	Range: 2.597(2)–2.609(2)		
Shortest relevant intermolecular distances			
BEDO-TTF/PhCN		*BEDO-TTF/BEDO-TTF*	
N2–H10A	2.71(2)	O2–O4	3.07(2)
N2–H1B	2.75(2)	O1–O3	3.19(2)
N1–H1B	2.65(2)	S3–O1	3.61(6)
N1–S3	3.31(2)	S2–O4	3.86(5)
		S1–S3	5.57(8)
		S2–S4	5.75(7)
Cluster unit/BEDO-TTF		*PhCN/PhCN*	
Br5–H10B	3.02(2)	N1–H26	2.49(2)
Br1–H9A	3.03(3)		
Br3–C7	3.47(2)		
Br2–C4	3.51(2)		

discussed by comparison with related compounds obtained with I_3^- or $[Mo_6Cl_{14}]^{2-}$ anions associated with chalcogenafulvalenoid electron donors.

2. Experimental section

2.1. Synthesis

$(Bu_4N)_2Mo_6Br_{14}$ was used as cluster precursor and was synthesized according to the procedure described in [6]. Typically, 10 mg (3.16×10^{-2} mmol) of BEDO-TTF and 100 mg (4.58×10^{-2} mmol) of $(Bu_4N)Mo_6Br_{14}$ were dissolved in benzonitrile and subsequently introduced in an 18 mL glass cell. $(BEDO\text{-}TTF)_2Mo_6Br_{14}(PhCN)_4$ was obtained under the form of crystalline powder by conventional electro-oxidation method under constant current of 0.5 μA at 10 °C. Suitable single crystals for X-ray diffraction studies were obtained directly during such syntheses.

2.2. Determination of the crystal structure

Single-crystal X-ray diffraction data of $(BEDO\text{-}TTF)_2Mo_6Br_{14}(PhCN)_4$ were collected at room temperature on a Mac Science MXC$^\chi$ X-ray diffractometer using Mo$K\alpha$ radiation ($\lambda = 0.71073$ Å). Empirical absorption correction was applied based on psi-scan data. Details of data collections and structure refinements are reported in Table 1. The data were processed by the Crystan analysis software [12]. Among the possible space groups deduced from the observed systematic extinctions, the refinement procedure allowed to retain the $P2_1/n$ centrosymmetric space group. The structure was solved by direct methods using SHELXS-97 program [13]. Subsequent structural refinements by least-squares techniques, combined with Fourier difference syntheses, were performed using SHELXL-97 program [14]. Hydrogen atoms were generated by SHELX program; their positions and atomic displacement parameters were not refined. All of the atoms are located on 4*e* Wyckoff crystallographic positions and the nonhydrogen atoms have been refined anisotropically. The atomic positional parameters and the equivalent displacement parameters are reported in Table 2. Relevant interatomic distances for discussion are reported in Table 3.

Crystallographic data (excluding structure factors) for the structure reported in this paper have been deposited with the Cambridge Crystallographic Data Center as supplementary publication no. CCDC__293170. Copies of the data can be obtained free of charge on application to CCDC, 12 Union Road, Cambridge CB2 1EZ, UK (fax: (44) 1223 336-033; e-mail: deposit@ccdc.cam.ac.uk).

3. Results and discussion

3.1. Crystal structure of $(BEDO\text{-}TTF)_2Mo_6Br_{14}(PhCN)_4$

$(BEDO\text{-}TTF)_2Mo_6Br_{14}(PhCN)_4$ crystallizes in the monoclinic system (Fig. 1), space group $P2_1/n$ ($a = 10.414(4)$ Å, $b = 21.711(7)$ Å, $c = 15.958(5)$ Å, $\beta = 93.65(3)^\circ$, $V = 3601(2)$ Å^3, $Z = 2$). The average Mo-Mo, Mo–Br^i and Mo–Br^a interatomic distances within the $[Mo_6Br_8^iBr_6^a]^{2-}$ discrete anionic unit are in agreement with those reported for other $A_xMo_6Br_{14}$ bromides and in particular with those of the $(Bu_4N)_2Mo_6Br_{14}$ starting compound (2.638, 2.603, 2.594 versus 2.635, 2.601 and 2.600 Å, respectively) [6]. The $[Mo_6Br_{14}]^{2-}$ units are aligned along the *a*-axis with inter-cluster distances of 10.414 Å (centroid to centroid) close to that found in $Cs_2Mo_6Br_{14}$ (10.192 Å) [6a] and without any contacts between halogen ligands (Fig. 2). The benzonitrile solvent molecules are located between the unit alignments leading to larger inter-cluster

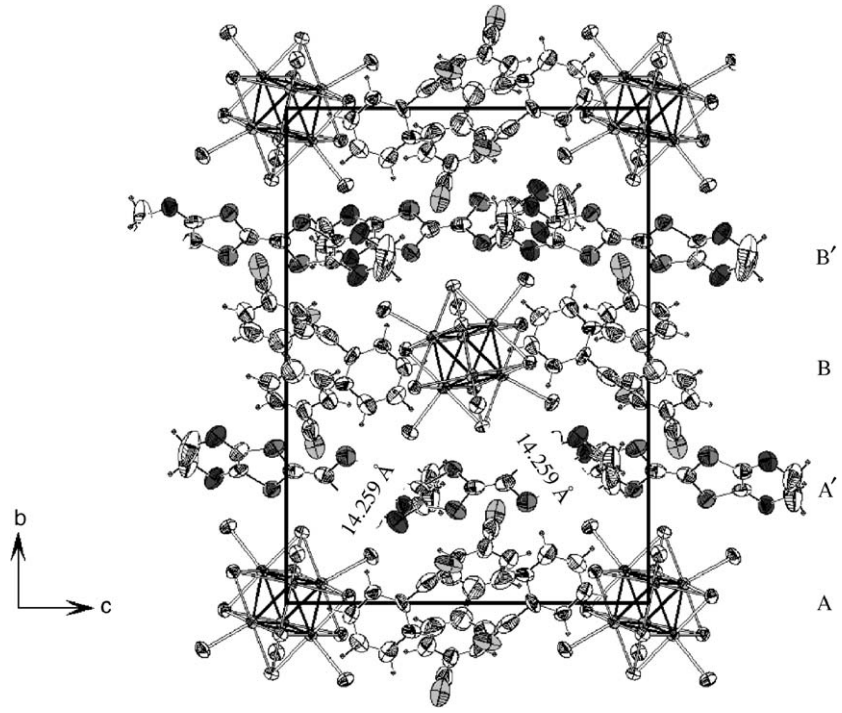

Fig. 1. Representation of the crystal structure of $(BEDO\text{-}TTF)_2Mo_6Br_{14}(PhCN)_4$, projection along [100]. Displacement ellipsoids are shown at the 50% probability level.

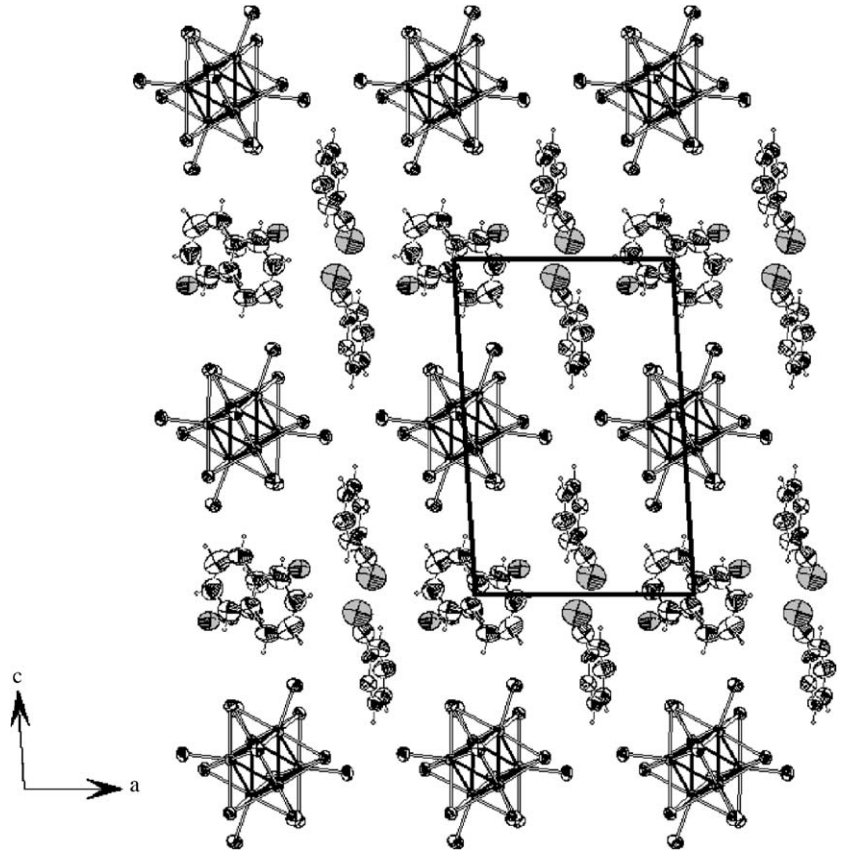

Fig. 2. Representation of the cluster and benzonitrile layer, projection along [010], $b = 1/2$. Displacement ellipsoids are shown at the 50% probability level.

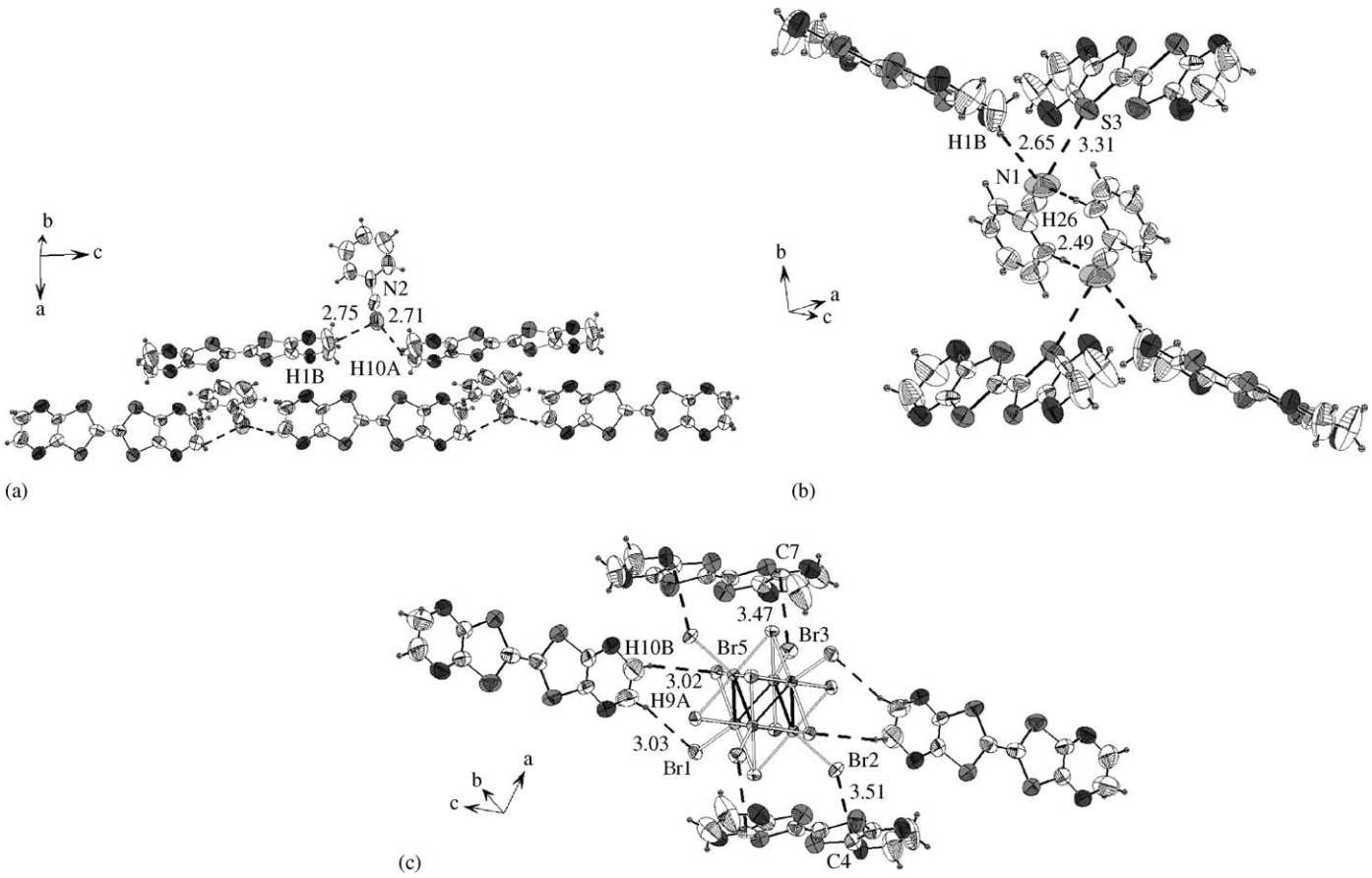

Fig. 3. (a) Representation of the intermolecular contacts (dashed lines) between benzonitrile and BEDO-TTF molecules. (b) Environment of the paired benzonitrile molecules by BEDO-TTF molecules. (c) Environment of the $[Mo_6Br_{14}]^{2-}$ cluster unit by BEDO-TTF molecules. All displacement ellipsoids are shown at the 50% probability level.

distances of 15.958 Å along the *c*-direction within the *ac* plane. The layers built up from anionic units and solvent molecules are stacked along the *b*-direction according to an *A–B–A* mode. Layers of $[BEDO\text{-}TTF]^+$ cationic entities are located between the clusters unit layers and stacked according to an *A′–B′–A′* sequence. They are organized in quincunx parallel to the *c* axis. Finally, the association of the two stackings along the *b*-direction leads to an *A–A′–B–B′* succession of planes (Fig. 1). The inter-cluster distances between the clusters of two successive unit layers are 14.259 and 14.626 Å. The structure can be conveniently depicted as a cationic organic tridimensional framework built up from $[BEDO\text{-}TTF]^+$ and PhCN in which is embedded the $[Mo_6Br_{14}]^{2-}$ inorganic unit. For the discussion, the van der Waals radii have been taken from Ref.[15]. Therefore, the van der Waals radii sum is 2.75, 3.35, 3.55 and 3.05 Å for N⋯H, N⋯S, C⋯Br and H⋯Br contacts respectively. Two crystallographically independent benzonitrile molecules, represented on Figs. 3a and b, act as linkers between the $[BEDO\text{-}TTF]^+$ cations. The first one ensures the linkage between the $[BEDO\text{-}TTF]^+$ cations within the *ac* plane to build organic chains (Fig. 3a) via C–H⋯N2 intermolecular contacts (2.749 Å (C–H1B⋯N2) and 2.715 Å (C–H10B⋯N2)) equal the van der Waals radii sum (2.75 Å). The second one builds a pair with another benzonitrile molecule with C–H26⋯N1 intermolecular distances (2.49 Å) shorter than the sum of the van der Waals radii that can be thus assimilated to hydrogen bonds. This pair of benzonitrile is located between four $[BEDO\text{-}TTF]^+$ cations and serves as linker between the chains of $[BEDO–TTF]^+$ (Fig. 3b). The C–H1B⋯N1 and N1⋯S3 intermolecular atomic contacts between PhCN and $[BEDO\text{-}TTF]^+$ (2.646 and 3.314 Å, respectively) are roughly equal to the sum of the van der Waals radii. This cationic organic framework is characterized by large cavities in which are embedded the units. Each cluster unit is surrounded by four radical molecules (Fig. 3c). Two of the four radicals exhibit short $C\cdots Br^a$ intermolecular contacts with the cluster units (C7⋯Br3 (3.47(2) Å) and C4⋯Br2 (3.51(2) Å)), shorter than van der Waals radii sum. The two other radicals exhibit $H\cdots Br^a$ and $H\cdots Br^i$ intermolecular contacts with the cluster unit (H10B⋯Br5 (3.02(2) Å) and H9A⋯Br1 (3.03(3) Å)), roughly equal to the van der Waals radii sum. Let us point out that the solvent molecules are not involved in the coordination of the units. It is noteworthy that the $[BEDO\text{-}TTF]^+$ monocations are not dimerized in $(BEDO\text{-}TTF)_2Mo_6Br_{14}(PhCN)_4$ as usually observed with other counter anions

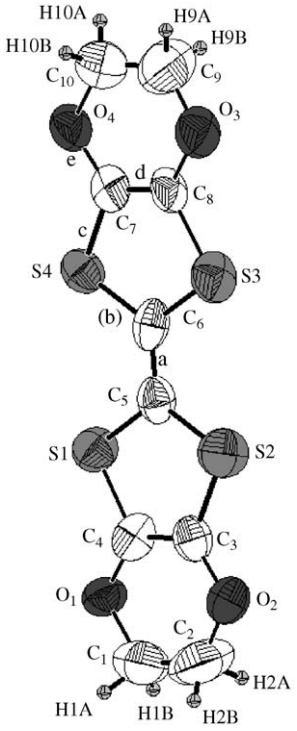

Fig. 4. Representation of the BEDO-TTF molecule. The a, b, c, d and e labels refer to the bonds reported in Table 4. All displacement ellipsoids are shown at the 50% probability level.

as for instance I_3^- in (BEDO-TTF)I_3 [16]. The S···S, S···O and O···O intermolecular distances (5.75(7), 3.86(5) and 3.07(2) Å respectively) are too long to enable the overlap between radical orbitals. This feature has been confirmed by the calculated overlap integrals [17] between neighboring BEDO-TTF molecules. In addition to absorption and magnetic measurements (see below), the oxidation state of these radicals (+1) has been corroborated by the values of characteristic intramolecular distances (Fig. 4 and Table 4).

The association of BEDO-TTF with I_3^- anion has previously led to a set of structures in which the BEDO-TTF entity exhibits various stacking and oxidation states. For instance, in (BEDO-TTF)I_3 [16], the monocationic radicals of [BEDO-TTF]$^+$ are eclipsed with an almost face-to-face overlap and the conducting band is half-filled. It results in a dimerization of [BEDO-TTF]$^+$ with a band gap at the Fermi level. Thus, this compound is an electrical insulator and exhibits a diamagnetic behavior. In (BEDO-TTF$^{+0.42}$)$_{2.4}I_3$ [18], the overlapping of radicals occurs in slipped manner along the lateral direction of the molecule. The conducting band being partially filled, it results in a metallic conductor behavior. Owing to the self-assembling nature of partially charged BEDO-TTF molecules, similar overlapping modes are frequently observed in BEDO-TTF based salts [16]. The origins of their self-assembling nature are intermolecular C–H···O hydrogen bonds and stabilization effect of wide conduction band formation that does not occur in mono- and di-cationic BEDO-TTF salts. In

Table 4
Mean bond lengths of BEDO-TTF molecules at different oxidation states (Å): BEDO-TTF (I), (BEDO-TTF)I_3 (II), (BEDO-TTF)$_2Mo_6Br_{14}$(PhCN)$_4$ (III), (BEDO-TTF)$(I_3)_2$ (IV)

	I	II	III	IV
Ref.	[16]	[16]	This work	[16]
Oxidation state	0	+1	+1	+2
Bond (a)	1.357	1.398	1.37(2)	1.427
Bond (b)	1.762	1.723	1.71(2)	1.702
Bond (c)	1.754	1.727	1.75(2)	1.702
Bond (d)	1.333	1.350	1.31(2)	1.420
Bond (e)	1.368	1.365	1.33(2)	1.309

Bonds a, b, c, d and e refer to representation of Fig. 4.

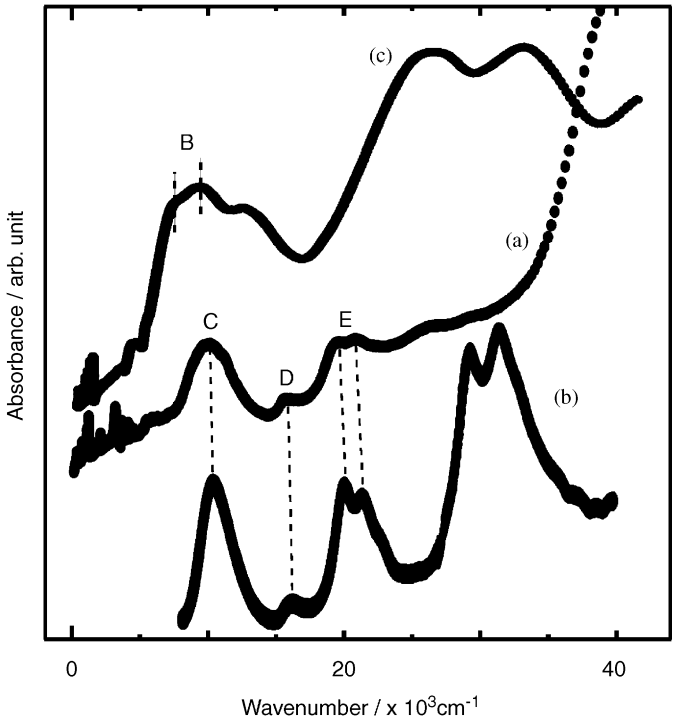

Fig. 5. UV–VIS–NIR absorption spectra of (a) (BEDO-TTF)$_2Mo_6Br_{14}$(PhCN)$_4$ in KBr pellet, (b) (BEDO-TTF)$_2Br(H_2O)_3$ in methanol and (c) (BEDO-TTF)I_3 in KBr pellet. The split band at around 30×10^3 cm^{-1} in curve b is ascribed to the intramolecular transition of neutral BEDO-TTF molecule generated by the dissociation of the Br salt in methanol: (BEDO-TTF$^{0.5+}$)$_2 \rightarrow$ BEDO-TTF$^{+\bullet}$ + BEDO-TTF^0.

(BEDO-TTF^{2+})$(I_3)_2$, discrete BEDO-TTF are encountered [16] but with fully [BEDO-TTF]$^{2+}$ oxidized dicationic radicals. This compound exhibits then electrical insulating and diamagnetic properties.

In Table 4 are reported the relevant bond lengths within the BEDO-TTF molecule for the title compound as well as those found in BEDO-TTF^0, (BEDO-TTF^{+1})I_3 and (BEDO-TTF^{+2})$(I_3)_2$. The bond lengths in (BEDO-TTF)$_2Mo_6Br_{14}$(PhCN)$_4$ are close to those found in (BEDO-TTF)I_3 in which the oxidation state is also +1.

This finding evidences that the dimerization of the monocationic radicals does not affect significantly the intramolecular bond-lengths. On the other hand and as previously reported [16], the analysis of the distances of Table 4, evidences that within the BEDO-TTF molecule the intramolecular bond lengths depend on its oxidation state. Indeed, as the oxidation state increases, C–S and C–O bond lengths decrease and C=C bond lengths increase (see Table 4).

The parent hybrid $(TMTTF^{+1})_2Mo_6Cl_{14}$ has been previously reported in the literature [7(a),7(b)]. In this compound, the TMTTF cations (TMTTF = tetramethyltetrathiafulvalene) are arranged into columns and are dimerized in a similar way to that observed in (BEDO-TTF^{+1})I_3. In $(BEDO\text{-}TTF)_2Mo_6Br_{14}(PhCN)_4$, the anionic unit and the additional benzonitrile seem to have a strong influence in the arrangement of the BEDO-TTF preventing the overlap between these radicals.

3.2. UV–VIS–NIR absorption spectra

The UV–VIS–NIR absorption spectra have been recorded on a SHIMADZU UV-3100 spectrometer and are reported in Fig. 5. The band-C, which was attributed to the intramolecular transition from SOMO-1 to SOMO of BEDO-TTF cation radical molecule [11], was clearly observed at $10.4\times10^3\,cm^{-1}$ in the UV-VIS-NIR absorption spectrum of $(BEDO\text{-}TTF)_2Mo_6Br_{14}(PhCN)_4$ (curve a). The spectrum is in excellent agreement with that observed for the monomeric form of BEDO-TTF cation radical (curve b), but differs considerably from that of segregated solid of BEDO-TTF cation radicals (curve c). The monomeric form of BEDO-TTF cation radical exhibits intramolecular absorption bands at 10.6 (band C), 16.6 (band D), 20.4 and $21.7\times10^3\,cm^{-1}$ (band E), whilst (BEDO-TTF^+)I_3 displays the intra- and interdimer transitions in a segregated column of BEDO-TTF^+ at 7.8 and $9.8\times10^3\,cm^{-1}$, respectively (band B in curve c). The characteristic absorption bands for the intermolecular transition for partial ionized (below $5\times10^3\,cm^{-1}$) and completely ionized BEDO-TTF molecules (band B) in a segregated column [19], were not observed at below $10\times10^3\,cm^{-1}$ in curve a. The spectrum is consistent with the crystal structure based on non-dimerized BEDO-TTF radical cation molecules.

3.3. Magnetic properties of $(BEDO\text{-}TTF)_2Mo_6Br_{14}(PhCN)_4$

The magnetic susceptibility of $(BEDO\text{-}TTF)_2Mo_6Br_{14}(PhCN)_4$ is recorded with a SQUID magnetosusceptometer (Quantum design MPMS) in the temperature range 2.0–300 K. The plot of the product of the magnetic susceptibility (χ) by the temperature (T), versus temperature, is reported in Fig. 6. The Pascal diamagnetism of $[Mo_6Br_{14}]^{2-}$ was evaluated as -1.94×10^{-4} emu/mol based on the susceptibility measurements on $(Bu_4N)_2Mo_6Br_{14}$ (-5.88×10^{-4} emu/mol) and $(Bu_4N)Br$ (-2.33×10^{-4} emu/mol). It was well fitted by Curie–Weiss law with $C=0.37\pm0.1$ emu/(spin of BEDO-TTF) K and $\Theta=-4.2$ K in the range of 60–300 K. The Curie constant is close to that of independent $S=1/2$ spin ($C=0.375$) and it

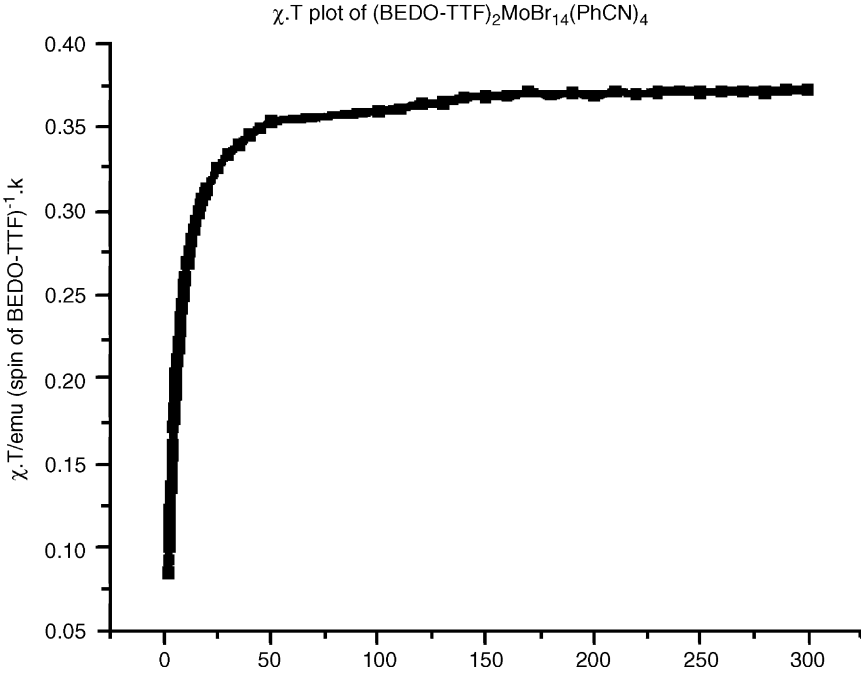

Fig. 6. Plot of the magnetic susceptibility (χ) by the temperature (T), χT, versus temperature, of $(BEDO\text{-}TTF)_2Mo_6Br_{14}(PhCN)_4$. The magnetic susceptibilities are measured by a SQUID magnetometer at the field of 2000 Oe.

is consistent with its crystal structure, more precisely with the presence of magnetic $[BEDO\text{-}TTF]^{+}$ radical molecules and diamagnetic $[Mo_6Br_{14}]^{2-}$ units with $24e^{-}$ per Mo_6 cluster. The small Weiss constant is also consistent with the small intermolecular overlap integrals among non-interacting and non- dimerized BEDO-TTF molecules. Below 50 K, the χT values decrease with lowering temperature due to weak antiferromagnetic interactions among BEDO-TTF radical molecules.

4. Conclusion

$(BEDO\text{-}TTF)_2Mo_6Br_{14}(PhCN)_4$ is the first charge transfer salt based on non- dimerized $[BEDO\text{-}TTF]^{+}$ monocationic radical (BEDO-TTF = bis(ethylenedioxy) tetrathiafulvalene). This non-dimerization was possible using $[Mo_6Br_{14}]^{2-}$ cluster unit as counter anion. The $[Mo_6Br_{14}]^{2-}$ inorganic unit is embedded in a cationic organic three-dimensional framework built up from BEDO-TTF and PhCN molecules, held together by the aid of C–H···N, N···S and N···H intermolecular contacts. Such an arrangement prevents overlapping between $[BEDO\text{-}TTF]^{+}$ monocationic radicals. The interatomic distances within the discrete $[BEDO\text{-}TTF]^{+}$ in $(BEDO\text{-}TTF)_2Mo_6Br_{14}(PhCN)_4$ are close to that found in $(BEDO\text{-}TTF^{+1})I_3$ in which the $[BEDO\text{-}TTF]^{+}$ radicals are dimerized. Anionic cluster units could be further used as 'template' for the design of new organic framework whose cavities will be controlled by the cluster unit radii size. The short intermolecular $Br^{a}\cdots C$ contacts between $[Mo_6Br_{14}]^{2-}$ and $[BEDO\text{-}TTF]^{+}$ observed in the title compound could lead to magnetic interactions replacing the diamagnetic $[Mo_6Br_{14}]^{2-}$ ($24\,e^{-}/Mo_6$) by a magnetic one as for instance $[Mo_6Br_7SCl_6]^{2-}$ ($23\,e^{-}/Mo_6$) obtained in $(Bu_4N)_3Mo_6Br_7SCl_6$ [20].

Acknowledgments

This work has been supported in part by a research grant from the French Ministry of Research and Education for KK, by a PICS contract 1433 from CNRS, by Fondation Langlois, by a COE Research on Elements Science (No.12CE2005) and a Grant-in-Aid (21st Century COE programs on Kyoto University Alliance for Chemistry and 15205019) from the Ministry of Education, Culture, Sports, Science and Technology, Japan.

References

[1] H. Schäfer, H.-G. von Schnering, Angew. Chem. 76 (1964) 833.
[2] C. Perrin, J. Alloys Compd. 262 (1997) 10.
[3] R. Chevrel, M. Sergent, Superconductivity in ternary compounds, in: Ø. Fischer, M.P. Maple (Eds.), Topics in Current Physics, Springer, Berlin, Heidelberg, New York, 1982.
[4] P. Braunstein, L.A. Oro, P.R. Raithby (Eds.), Metal Clusters in Chemistry, vol. II, Wiley-VCH, Weinheim, 1999.
[5] J.M. Tarascon, F.J. Di Salvo, D.W. Murphy, G.W. Hull, E.A. Rietman, S.V. Waszczak, J. Solid State Chem. 54 (1984) 104.
[6] (a) K. Kirakci, S. Cordier, C. Perrin, Z. Anorg. Allg. Chem. 631 (2005) 411;
(b) K. Kirakci, S. Cordier, T. Roisnel, S. Golhen, C. Perrin, Z. Kristallogr.— NCS 220 (2005) 116.
[7] (a) P. Batail, L. Ouahab, Mol. Cryst. Liq. Cryst. 125 (1985) 205;
(b) L. Ouahab, P. Batail, C. Perrin, C. Garrigou-Lagrange, Mat. Res. Bull. 21 (1986) 1223;
(c) A. Deluzet, P. Batail, Y. Misaki, P. Auban-Senzier, E. Canadell, Adv. Mater. 12 (2000) 436.
[8] (a) D.H. Johnston, D.C. Gaswick, M.C. Lonergan, C.L. Stern, D.F. Shriver, Inorg. Chem. 31 (1992) 1869;
(b) N. Prokopuk, D. Shriver, Inorg. Chem. 36 (1997) 5609;
(c) C.B. Gorman, W.Y. Su, C.M. Watson, P. Boyle, Chem. Comm. (1999) 877.
[9] (a) S. Cordier, K. Kirakci, D. Méry, C. Perrin, D. Astruc, Inorg. Chim. Acta 359 (2006) 1705;
(b) D. Méry, C. Ornelas, M.-C. Daniel, J. Ruiz, J. Rodrigues, D. Astruc, S. Cordier, K. Kirakci, C. Perrin, C. R. Chimie 8 (2005) 1789.
[10] G. Pilet, K. Kirakci, F. de Montigny, S. Cordier, C. Lapinte, C. Perrin, A. Perrin, Eur. J. Inorg. Chem. 5 (2005) 919.
[11] S. Horiuchi, H. Yamochi, G. Saito, K. Sakaguchi, M. Kusunoki, J. Am. Chem. Soc. 118 (1996) 8604.
[12] Gilmore and Brown, CRYSTAN-GM, 1988.
[13] G.M. Sheldrick, SHELXS-97: Structure solution by Patterson and direct methods, University of Göttingen, Göttingen, 1997.
[14] G.M. Sheldrick, SHELXL-97: Program for the Refinement of Crystal Structure, University of Göttingen: Göttingen, 1997.
[15] A. Bondi, J. Phys. Chem. 68 (1964) 441.
[16] S. Horiuchi, H. Yamochi, G. Saito, K. Matsumoto, Mol. Cryst. Liq. Cryst. 284 (1996) 357.
[17] T. Mori, A. Kobayashi, Y. Sasaki, H. Kobayashi, G. Saito, H. Inokuchi, Bull. Chem. Soc. Japan. 57 (1984) 627.
[18] F. Wudl, H. Yamochi, T. Suzuki, H. Isotalo, C. Fite, H. Kasmai, K. Liou, G. Srdanov, J. Am. Chem. Soc. 112 (1990) 2461.
[19] (a) J.B. Torrance, Acc. Chem. Res. 12 (1979) 79;
(b) T. Senga, K. Kamoshida, L.A. Kushch, G. Saito, T. Inamoto, I. Ono, Mol. Cryst. Liq. Cryst. 296 (1997) 97.
[20] M. Ebihara, K. Isobe, K. Saito, Inorg. Chem. 31 (1992) 1644.